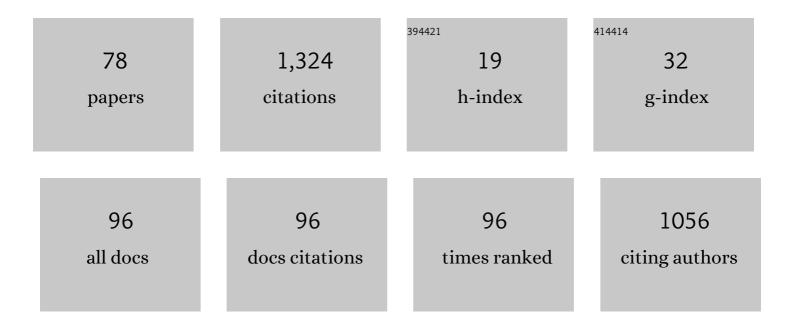
Giovanni Bianchini

List of Publications by Year in descending order

Source: https://exaly.com/author-pdf/4981458/publications.pdf Version: 2024-02-01



#	Article	IF	CITATIONS
1	The FORUM end-to-end simulator project: architecture and results. Atmospheric Measurement Techniques, 2022, 15, 573-604.	3.1	9
2	Observations of the downwelling far-infrared atmospheric emission at the Zugspitze observatory. Earth System Science Data, 2021, 13, 4303-4312.	9.9	9
3	lce and mixed-phase cloud statistics on the Antarctic Plateau. Atmospheric Chemistry and Physics, 2021, 21, 13811-13833.	4.9	11
4	Far-Infrared Radiation Mobile Observation System for ground and balloon-borne validation of the FORUM mission. , 2021, , .		0
5	Comparison of mid-latitude single- and mixed-phase cloud optical depth from co-located infrared spectrometer and backscatter lidar measurements. Atmospheric Measurement Techniques, 2021, 14, 6749-6758.	3.1	3
6	Characterization of the Far Infrared Properties and Radiative Forcing of Antarctic Ice and Water Clouds Exploiting the Spectrometer-LiDAR Synergy. Remote Sensing, 2020, 12, 3574.	4.0	9
7	The two-stream δ-Eddington approximation to simulate the far infrared Earth spectrum for the simultaneous atmospheric and cloud retrieval. Journal of Quantitative Spectroscopy and Radiative Transfer, 2020, 246, 106927.	2.3	8
8	Can downwelling far-infrared radiances over Antarctica be estimated from mid-infrared information?. Atmospheric Chemistry and Physics, 2019, 19, 7927-7937.	4.9	3
9	Antarctic Ice Cloud Identification and Properties Using Downwelling Spectral Radiance From 100 to 1,400 cm ^{âr'1} . Journal of Geophysical Research D: Atmospheres, 2019, 124, 4761-4781.	3.3	14
10	Analysis of Water Vapor Absorption in the Farâ€Infrared and Submillimeter Regions Using Surface Radiometric Measurements From Extremely Dry Locations. Journal of Geophysical Research D: Atmospheres, 2019, 124, 8134-8160.	3.3	26
11	A Fourier transform spectroradiometer for ground-based remote sensing of the atmospheric downwelling long-wave radiance. Atmospheric Measurement Techniques, 2019, 12, 619-635.	3.1	20
12	Spectral characterization of the surface longwave radiation over the East Antarctic Plateau. AIP Conference Proceedings, 2017, , .	0.4	1
13	Simultaneous retrieval of water vapour, temperature and cirrus clouds properties from measurements of far infrared spectral radiance over the Antarctic Plateau. Atmospheric Measurement Techniques, 2017, 10, 825-837.	3.1	18
14	The Far Infrared FTS for the FORUM Mission. , 2016, , .		3
15	Remote sensing of cirrus cloud microphysical properties using spectral measurements over the full range of their thermal emission. Journal of Geophysical Research D: Atmospheres, 2016, 121, 10,804.	3.3	22
16	One year of downwelling spectral radiance measurements from 100 to 1400 cm ^{â^'1} at Dome Concordia: Results in clear conditions. Journal of Geophysical Research D: Atmospheres, 2016, 121, 10,937.	3.3	5
17	Two years of spectrally-resolved measurements of the Antarctic downwelling atmospheric radiance within the COMPASS project. , 2016, , .		1
18	Far–IR Spectral Observations of the Earth's Longwave Radiation and Their Role in Climate Studies. , 2016		0

Fara€ IR Sp 2016, , .

GIOVANNI BIANCHINI

#	Article	IF	CITATIONS
19	Retrieval of Antarctic Cirrus Cloud Micro-Physics from Measurements of Far Infrared Spectral Radiance. , 2016, , .		Ο
20	Far-Infrared Radiative Properties of Water Vapor and Clouds in Antarctica. Bulletin of the American Meteorological Society, 2015, 96, 1505-1518.	3.3	32
21	Radiometric calibration of the Radiation Explorer in the Far InfraRed prototype. , 2015, , .		Ο
22	A Fourier Transform Spectroradiometer for the Remote Sensing of the Atmospheric Emission from Ground Bases in Extreme Environments. , 2015, , .		0
23	Validation of H_2O continuum absorption models in the wave number range 180–600 cm^â"1 with atmospheric emitted spectral radiance measured at the Antarctica Dome-C site. Optics Express, 2014, 22, 16784.	3.4	24
24	Measurement of the thermal expansion coefficient of AISI 420 stainless steel between 20 and 293K. Cryogenics, 2014, 62, 94-96.	1.7	11
25	Analysis of cirrus cloud spectral signatures in the far infrared. Journal of Quantitative Spectroscopy and Radiative Transfer, 2014, 141, 49-64.	2.3	19
26	A novel interferometric dilatometer in the 4–300 K temperature range: thermal expansion coefficient of SRM-731 borosilicate glass and stainless steel-304. Measurement Science and Technology, 2013, 24, 105203.	2.6	11
27	Characterization of the Radiative Properties of Cirrus Clouds With a Wide-band Fourier Transform Spectroradiometer. , 2013, , .		0
28	Groundâ€based high spectral resolution observations of the entire terrestrial spectrum under extremely dry conditions. Geophysical Research Letters, 2012, 39, .	4.0	24
29	Water vapor sounding with the far infrared REFIR-PAD spectroradiometer from a high-altitude ground-based station during the ECOWAR campaign. Journal of Geophysical Research, 2011, 116, .	3.3	15
30	The REFIR-PAD far-infrared Fourier transform spectroradiometer. , 2011, , .		1
31	Wideband far infrared FTS for the FORUM explorer mission. , 2011, , .		Ο
32	An Intercomparison of Precipitable Water Vapor Measurements Obtained During the ECOWAR Field Campaign. , 2009, , .		0
33	Groundâ€Based and Balloonâ€Borne Characterization of the Far Infrared Atmospheric Emission Spectrum. , 2009, , .		Ο
34	Vectorial combination of signals in Fourier transform spectroscopy. Infrared Physics and Technology, 2009, 52, 19-21.	2.9	9
35	Validation of version-4.61 methane and nitrous oxide observed by MIPAS. Atmospheric Chemistry and Physics, 2009, 9, 413-442.	4.9	50
36	Test of far-infrared atmospheric spectroscopy using wide-band balloon-borne measurements of the upwelling radiance. Journal of Quantitative Spectroscopy and Radiative Transfer, 2008, 109, 1030-1042.	2.3	18

GIOVANNI BIANCHINI

#	Article	IF	CITATIONS
37	Design and characterisation of black-body sources for infrared wide-band Fourier transform spectroscopy. Infrared Physics and Technology, 2008, 51, 207-215.	2.9	15
38	Spectrally resolved observations of atmospheric emitted radiance in the H2O rotation band. Geophysical Research Letters, 2008, 35, .	4.0	42
39	Retrieval of foreign-broadened water vapor continuum coefficients from emitted spectral radiance in the H_2O rotational band from 240 to 590 cm^-1. Optics Express, 2008, 16, 15816.	3.4	39
40	Measurements of low amounts of precipitable water vapor by millimeter wave spectroscopy: An intercomparison with radiosonde, Raman lidar, and Fourier transform infrared data. Journal of Geophysical Research, 2008, 113, .	3.3	20
41	Measurement of the water vapour vertical profile and of the Earth's outgoing far infrared flux. Atmospheric Chemistry and Physics, 2008, 8, 2885-2894.	4.9	37
42	Technical Note: REFIR-PAD level 1 data analysis and performance characterization. Atmospheric Chemistry and Physics, 2008, 8, 3817-3826.	4.9	21
43	Characterization of tropical atmosphere through wide-band emission spectra acquired with a balloon-borne uncooled FTS spectroradiometer. Proceedings of SPIE, 2007, , .	0.8	1
44	Geophysical validation of MIPAS-ENVISAT operational ozone data. Atmospheric Chemistry and Physics, 2007, 7, 4807-4867.	4.9	130
45	Validation of MIPAS HNO ₃ operational data. Atmospheric Chemistry and Physics, 2007, 7, 4905-4934.	4.9	48
46	Far-infrared spectrally resolved broadband emission of the atmosphere from Morello and Gomito mountains near Florence. , 2007, , .		3
47	REFIR/BB initial observations in the water vapour rotational band: Results from a field campaign. Journal of Quantitative Spectroscopy and Radiative Transfer, 2007, 103, 524-535.	2.3	8
48	Interferometric dilatometer for thermal expansion coefficient determination in the 4–300 K range. Measurement Science and Technology, 2006, 17, 689-694.	2.6	20
49	Validation of MIPAS satellite measurements of HNO3using comparison of rotational and vibrational spectroscopy. Journal of Geophysical Research, 2006, 111, .	3.3	19
50	Infrared Balloon Experiment: improved instrumental configuration and assessment of instrument performance. Applied Optics, 2006, 45, 1041.	2.1	7
51	Technical note: First spectral measurement of the Earth's upwelling emission using an uncooled wideband Fourier transform spectrometer. Atmospheric Chemistry and Physics, 2006, 6, 5025-5030.	4.9	30
52	Wide-band spectrally resolved measurement of the Earth's up-welling radiation with the REFIR-PAD spectroradiometer. , 2006, , .		6
53	Frictionless mirror drive for intermediate resolution infrared Fourier transform spectroscopy. Infrared Physics and Technology, 2006, 48, 217-222.	2.9	3
54	A wide-band nadir-sounding spectroradiometer for the characterization of the Earth's outgoing long-wave radiation. , 2006, 6361, 62.		24

GIOVANNI ΒΙΑΝCΗΙΝΙ

#	Article	IF	CITATIONS
55	The Planetary Fourier Spectrometer (PFS) onboard the European Mars Express mission. Planetary and Space Science, 2005, 53, 963-974.	1.7	151
56	SAFIRE-A (spectroscopy of the atmosphere by using far-infrared emission-airborne): Assessment of measurement capabilities and future developments. Advances in Space Research, 2005, 36, 888-893.	2.6	0
57	Stratospheric minor gas distribution over the Antarctic Peninsula during the APE–GAIA campaign. International Journal of Remote Sensing, 2005, 26, 3343-3360.	2.9	5
58	Breadboard of a Fourier-transform spectrometer for the Radiation Explorer in the Far Infrared atmospheric mission. Applied Optics, 2005, 44, 2870.	2.1	35
59	The Broadband Fourier Transform Spectrometer for the REFIR (Radiation Explorer in the Far Infrared) Space Mission. , 2005, , .		0
60	Radiometric performances of the Fourier transform spectrometer for the Radiation Explorer in the Far-Infrared (REFIR) space mission. , 2004, , .		2
61	SAFIRE-A (spectroscopy of the atmosphere by far-infrared emission—airborne): optimized instrument configuration and new assessment of improved performance. Applied Optics, 2004, 43, 2962.	2.1	14
62	LOW-TEMPERATURE THERMAL CHARACTERIZATION OF SUPPORT MATERIAL FOR MASSIVE CRYOGENIC DETECTORS. , 2002, , .		0
63	Assessment of Detector Nonlinearity in Fourier Transform Spectroscopy. Applied Spectroscopy, 2002, 56, 271-274.	2.2	16
64	Cosmic-ray spikes localization and correction in FT spectrometer data. Infrared Physics and Technology, 2002, 43, 33-38.	2.9	6
65	Emission Fourier transform spectroscopy for the remote sensing of the atmosphere. Optics and Lasers in Engineering, 2002, 37, 187-202.	3.8	6
66	Far infrared FT spectroscopy of the atmosphere from balloon to aircraft platforms. , 2001, , .		0
67	Thermal expansion and thermal conductivity of glass-fibre reinforced nylon at low temperature. Cryogenics, 2000, 40, 465-467.	1.7	14
68	Characterisation of instrumental line shape distortions due to path difference dependent phase errors in a Fourier transform spectrometer. Infrared Physics and Technology, 2000, 41, 287-292.	2.9	10
69	Flight qualification of a diode laser for path difference determination of a high-resolution Fourier transform spectrometer. Applied Optics, 2000, 39, 962.	2.1	11
70	Measurement of the Helium23P0â^23P1Fine Structure Interval. Physical Review Letters, 1999, 82, 1112-1115.	7.8	70
71	Thermal expansion and thermal conductivity of Torlon at low temperatures. Cryogenics, 1999, 39, 481-484.	1.7	38
72	Dielectric properties of Stycast 1266 over the 0.07–300 K temperature range. Cryogenics, 1999, 39, 963-966.	1.7	12

5

#	Article	IF	CITATIONS
73	Wide-bandwidth frequency locking of a 1083-nm extended-cavity DBR diode laser to a high-finesse Fabry-Pérot resonator. Applied Physics B: Lasers and Optics, 1998, 66, 407-410.	2.2	7
74	Electromagnetically induced transparency in a RF discharge. European Physical Journal D, 1998, 1, 85-91.	1.3	0
75	Lineshapes for a pure three level system: quantum coherence effects on absorption and birefringence of helium. AIP Conference Proceedings, 1997, , .	0.4	Ο
76	Birefringence in electromagnetically induced transparency. Optics Letters, 1997, 22, 736.	3.3	32
77	PFS: A fourier spectrometer for the study of Martian atmosphere. Advances in Space Research, 1997, 19, 1277-1280.	2.6	28
78	Precision Spectroscopy of Helium and the Fine Structure Constant. , 0, , .		0